JOURNAL OF SPACECRAFT AND ROCKETS
Vol. 42, No. 5, September–October 2005

Simplified Vibration Model of Solid-Rocket Motor Coupled with Solid Propellant

Yuji Kohsetsu*
Japan Aerospace Exploration Agency, Ibaraki 305-8505, Japan

A simplified method for generating a structural vibration model of a solid-rocket motor (SRM) is proposed. This method can create an SRM coupled model between a compressible motor case and an incompressible solid propellant using two finite element methods. One is the ordinary displacement-base finite element method (D-FEM), and the other is the mixed finite element method (M-FEM). Solid propellant is a fully incompressible material with a Poisson's ratio of 0.5; therefore, the D-FEM cannot be applied because of the zero divide in the relation between stresses and strains. However, the M-FEM can treat incompressible materials. An SRM model generated by this method can be built into the total launch vehicle model to analyze the launch vehicle vibration.

Nomenclature

A = section area of beam model
E = Young's modulus
G = shearing modulus
H = nodal pressure vector, $\{h, h, \ldots, h\}$
h = nodal pressure of mixed finite element method
I = unit matrix
K = stiffness matrix
L = length of solid-rocket motor (SRM)
M = mass matrix
n = number of circumferential waves
q = generalized coordinate of the constrained normal mode by the Craig–Bampton[7] method
R = radius of SRM case
r = orthogonal base coordinates
T = coupling matrix between a propellant model and a motor case model
u = axial displacement
v = tangential displacement
w = radial displacement
$\boldsymbol{X}$ = nodal displacement vector, $\{\ldots, u, v, w, \beta \ldots\}$, for a motor case and $\{\ldots, u, v, w, h, \ldots\}$ for a propellant
β = rotation of meridian
ν = Poisson's ratio
ρ = mass density
Φ = eigenvectors in matrix form
ω = angular frequency

I. Introduction

SOLID-ROCKET boosters (SRB) are commonly used to augment the thrust of expendable launch vehicles (Fig. 1). The large SRB plays an important role in the structural dynamics of the launch vehicle. Therefore, a structural dynamic analysis of the entire launch vehicle requires appropriate fidelity of the SRB model. The SRB consists of several subsystems: the nose cone, the forward adapter, the solid-rocket motor (SRM), and the afterward adapter. The SRM, which has a motor case that stows a massive amount of solid propellant, produces coupling between the motor case and solid propellant. Therefore, the SRM is the most significant subsystem in terms of the overall SRB structural dynamics. The SRB assembled model is built into the launch vehicle model. A simple and reliable method for generating an SRM model is the subject of this paper. Solid propellant is a fully incompressible material[1] with a Poisson's ratio of 0.5. The ordinary displacement-base finite element method (D-FEM) cannot be applied due to the incompressibility constraint, but the mixed finite element method (M-FEM)[2] can be used to analyze the solid-propellant dynamic motion. However, the M-FEM leads to another problem in the numerical calculation process. This problem originates from the M-FEM itself, which yields some zero diagonal elements of the system stiffness matrix for fully incompressible materials (Poisson's ratio of 0.5). These zero diagonal elements will produce numerical instability in the eigenvalue calculation process. The standard techniques used to conduct an eigenvalue analysis are sophisticated.[3–5] Artificial compressibility, the penalty method, and the iteration method are techniques used to prevent numerical instability. However, each technique is approximated because the Poisson's ratio value may be 0.4999, not exactly 0.5, and, thus, none of the techniques is precise. Given this situation, we developed an exact algorithm[6] that can conduct an eigenvalue analysis of the incompressible material's equations of motion based on the M-FEM. Our algorithm provides numerical stability to the eigenvalue calculation and an exact treatment of a Poisson's ratio of 0.5.

A simplified method for generating an SRM model (Fig. 2) can be used to consider the coupling between the compressible motor case and the incompressible solid propellant. This method introduces two finite element methods (FEMs). One is the ordinary D-FEM, and the other is the M-FEM. The D-FEM is used to generate a motor case model, and the M-FEM to generate a solid-propellant model. Our philosophy of the SRM model generation is simple and very reliable. This proposed method uses the Craig–Bampton (CB) method[7] to reduce the size of the SRM component model. The overall SRM structure is subdivided into two substructures, the motor case and the solid propellant. The motor case model retains the physical coordinates, whereas the solid-propellant model is transformed into the generalized coordinates of the CB method, whose degrees of freedom (DOF) are much fewer than the original DOF. The primary feature of our proposed method is the introduction of a new algorithm for CB model generation. The new algorithm enables the CB method to perform an eigenvalue calculation of the solid propellant's equations of motion based on the M-FEM. This eigenvalue calculation algorithm provides numerical stability to a constrained normal modes calculation.

The following subjects are presented in this paper: 1) a simplified method for generating a structural vibration model of an SRM; 2) the application of this method to generate an axial vibration mathematical model of an SRM; 3) the SRM vibration properties

Presented as Paper 2004-1790 at the AIAA/ASME/ASCE/AHS/ASC 45th Structures, Structural Dynamics, and Materials Conference, Palm Springs, CA, 19–22 April 2004; received 24 June 2004; revision received 4 October 2004; accepted for publication 13 October 2004.

*Deputy Director, Space Systems Evaluation Engineering Group, Institute of Space Technology and Aeronautics. Member AIAA.

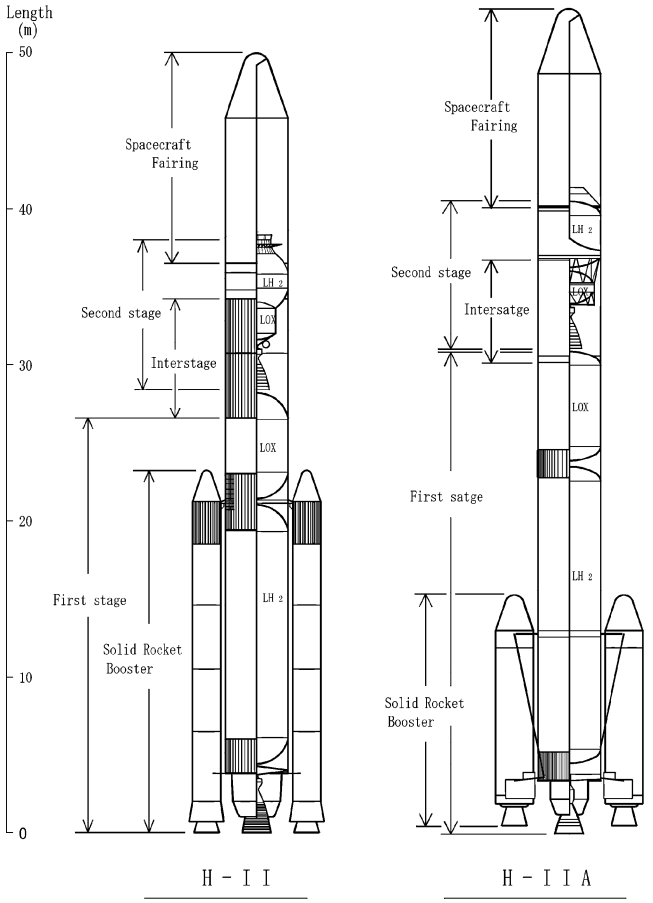

Fig. 1 Expendable launch vehicle configurations.

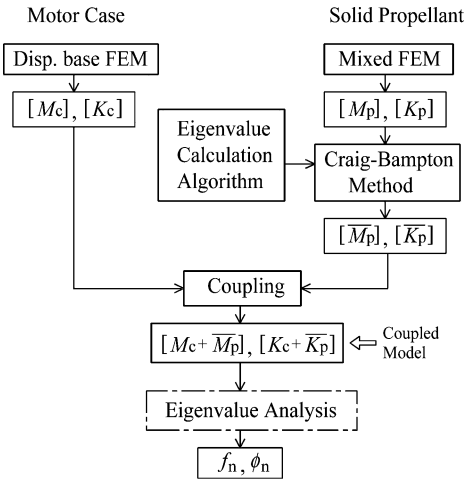

Fig. 2 Simplified method to generate an SRM model.

analyzed based on the exact incompressible condition, that is, Poisson's ratio = 0.5, and on a near-incompressible condition, that is, Poisson's ratio = 0.49, for a solid propellant; and 4) comparisons between the shell model and beam model for the SRM motor case substructure.

The Appendix briefly summarizes our eigenvalue calculation algorithm.[6] We assume a hypothetical SRM in item 2 with a length-to-radius ratio of 7.8 and generate a mathematical model of its axial vibration. Items 3 and 4 confirm that our proposed method of generating an SRM vibration model is simple and very reliable.

II. Strategy for Generating an SRM Model

The intention of our method is to create a model coupling the compressible motor case and the incompressible solid propellant.

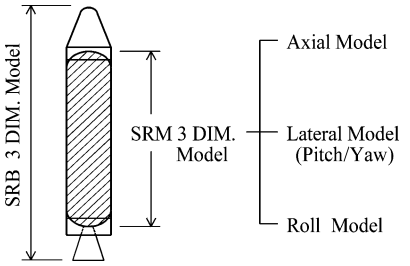

Fig. 3 Three-dimensional model construction.

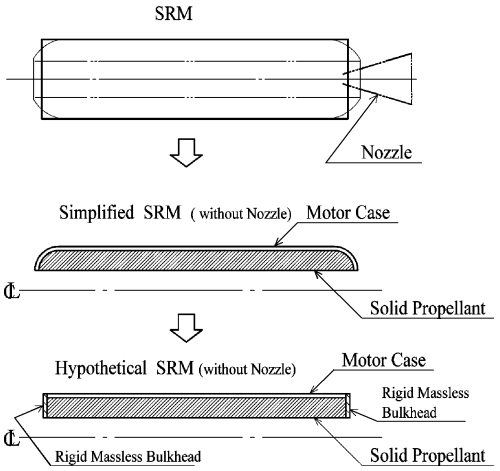

Fig. 4 Simplified SRM.

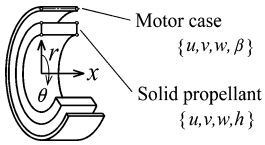

Fig. 5 Numerical analysis model.

An SRB three-dimensional vibration model, including the SRM model generated by this method, is to be built into a total launch vehicle model for conducting a launch vehicle vibration analysis. Our concept of SRM model generation is simple and very reliable. The SRM configuration can be assumed to be axisymmetric, and, thus, our simple concept leads to the proposal that a three-dimensional model of an SRM can be separated into three independent models, that is, an axial model, a lateral (pitch and yaw bending) model, and a roll (torsional) model (Fig. 3). Our method was designed to generate each independent model, but of course can also generate a three-dimensional model. We can simplify the configuration of an SRM and assume a hypothetical SRM (Fig. 4) with the propellant grain geometry of a circular port to describe the simplified method. This assumption does not degrade the theoretical basis of our method. This scheme uses the CB method to reduce the size of the SRM component model.

III. Simplified Method for Model Generation

A. Finite Element Model

The numerical analysis model is depicted in Fig. 5. An axisymmetric assumption can simplify model generation. The outer cylindrical shell is the motor case model, and the inner hollow cylinder is the solid-propellant model. Each model consists of axisymmetric elements. The motor case model uses a cylindrical shell ring element through the ordinary D-FEM. Each node has four DOF $\{u, v, w, \beta\}$. U, v, and w are the axial, tangential, and radial displacements, and β is the rotation of the meridian. The shape function of u and v is first order, and that of w is third order.

The propellant model uses a four-node quadrilateral section-ring element through the M-FEM. Each node has four degrees of freedom $\{u, v, w, h\}$. U, v, and w are the axial, tangential, and radial

displacements, and h is the pressure. The shape function for u, v, w, and h is first order. Therefore, a four-node element with an equal order of displacement and pressure field does not satisfy the Inf-Sup condition.[8] However, this is permissible because a structural dynamic study does not necessarily require pressure continuity. Moreover, the pressure DOF are eliminated by the CB method.

The separation of variables in the nodal displacements of the motor case and the solid propellant are expressed by Eqs. (1) and (2), respectively. Here, n is the number of circumferential waves, x is the axial coordinate, and θ is the angle of circumference coordinate:

$$u(x,\theta)=u(x)\cos n\theta, \qquad v(x,\theta)=v(x)\sin n\theta$$
$$w(x,\theta)=w(x)\cos n\theta, \qquad \beta(x,\theta)=\frac{\partial w(x,\theta)}{\partial x}=\frac{\partial w(x)}{\partial x}\cos n\theta \tag{1}$$

$$u(x,\theta)=u(x)\cos n\theta, \qquad v(x,\theta)=v(x)\sin n\theta$$
$$w(x,\theta)=w(x)\cos n\theta, \qquad h(x,\theta)=h(x)\cos n\theta \tag{2}$$

B. Motor Case

The D-FEM is applied to the motor case. The equation of vibration motion for the motor case is given by Eq. (3):

$$[M_c]\{\ddot{X}_c\}+[K_c]\{X_c\}=0 \tag{3}$$

Here, subscript c indicates the motor case and $\{X_c\}$ is the nodal displacement vector.

C. Solid Propellant

The M-FEM is applied to the solid propellant. The equation of the axisymmetric vibration motion is formulated because Eq. (4) based on the modified Hellinger–Reissner principle (see Ref. 9), which is equivalent to the Herrmann method.[1] The axisymmetric four-node ring element is used to express the solid-propellant vibration motion:

$$\begin{bmatrix} M_{pp} & 0 \\ 0 & 0 \end{bmatrix}\begin{Bmatrix} \ddot{X}_p \\ \ddot{H} \end{Bmatrix}+\begin{bmatrix} K_{pp} & K_{ph} \\ K_{ph}^T & K_{hh} \end{bmatrix}\begin{Bmatrix} X_p \\ H \end{Bmatrix}=0 \tag{4}$$

Here, subscript p indicates the solid propellant, and $\{X_p\}$ refers to the nodal displacement vectors. $\{H\}$ refers to the nodal pressure vectors. $[K_{hh}]$ becomes zero for full incompressibility (Poisson's ratio = 0.5).

$\{X_p, H\}^T$ is separated into the boundary coordinates and interior coordinates, as expressed by Eq. (5). Subscript b indicates the boundary DOF to interface with the motor case DOF, and subscript i indicates the interior DOF of the propellant based on the CB method:

$$\begin{aligned}\{X_p, H\}^T &= \{X_{pi}, H_i \vdots X_{pb}, H_b\}^T \\ &= \{X_{pi}, H_i, H_b \vdots X_{pb}\}^T \\ &\equiv \{X_{pi}, \bar{H}_i \vdots X_{pb}\}^T \\ &\equiv \{X_i \vdots X_b\}^T\end{aligned} \tag{5}$$

$\{H_b\}$ can be merged into $\{H_i\}$ because the motor case model has no DOF to constrain it. Thus, Eq. (4) is also subdivided to yield

$$\begin{bmatrix} M_{ii} & M_{ib} \\ M_{bi} & M_{bb} \end{bmatrix}\begin{Bmatrix} \ddot{X}_i \\ \ddot{X}_b \end{Bmatrix}+\begin{bmatrix} K_{ii} & K_{ib} \\ K_{bi} & K_{bb} \end{bmatrix}\begin{Bmatrix} X_i \\ X_b \end{Bmatrix}=0 \tag{6}$$

The calculations of the constrained normal modes are obtained from

$$[M_{ii}]\{\ddot{X}_i\}+[K_{ii}]\{X_i\}=0$$
$$\begin{bmatrix} M_{ii} & 0 \\ 0 & 0 \end{bmatrix}\begin{Bmatrix} \ddot{X}_{pi} \\ 0 \end{Bmatrix}+\begin{bmatrix} K_{iipp} & K_{iiph} \\ K_{iihp} & 0 \end{bmatrix}\begin{Bmatrix} X_{pi} \\ \bar{H}_i \end{Bmatrix}=0 \tag{7}$$

An eigenvalue analysis of Eq. (7) yields the constrained normal modes $[\Phi_n]$ as in Eq. (8). An algorithm developed[6] for eigenvalue calculation is used in this process:

$$\begin{Bmatrix} X_{pi} \\ \bar{H}_i \end{Bmatrix}=[\Phi_n]\{q_n\} \tag{8}$$

Here, $[\Phi_n]$ are eigenvectors and $\{q_n\}$ are the generalized coordinates by the constrained normal modes.

The constrained modes are calculated from

$$[K_{ii}]\{X_i\}+[K_{ib}]\{X_b\}=0$$
$$\begin{bmatrix} K_{ii,pp} & K_{ii,ph} \\ K_{ii,hp} & K_{ii,hh} \end{bmatrix}\begin{Bmatrix} X_{pi} \\ \bar{H}_i \end{Bmatrix}+\begin{bmatrix} K_{ib,pp} \\ K_{ib,hp} \end{bmatrix}\{X_b\}=0 \tag{9}$$

The constrained modes $[\Phi_c]$ are obtained as in Eq. (10) by solving $\{X_{pi}, \bar{H}_i\}^T$ from Eq. (9):

$$\begin{Bmatrix} X_{pi} \\ \bar{H}_i \end{Bmatrix}=[\Phi_c]\{X_b\} \tag{10}$$

A new coordinate transformation is defined as in Eq. (11) by the superposition of Eqs. (8) and (10):

$$\begin{Bmatrix} X_i \\ X_b \end{Bmatrix}=\begin{Bmatrix} X_i \\ \bar{H}_i \\ \hline X_b \end{Bmatrix}=\left[\begin{array}{c|c} \Phi_n & \Phi_c \\ \hline 0 & I \end{array}\right]\begin{Bmatrix} q_n \\ X_b \end{Bmatrix} \tag{11}$$

The constrained normal modes with higher frequencies in Eq. (11) can be truncated to reduce the propellant model size. An approximated coordinate transformation by Eq. (12) is then defined:

$$\begin{Bmatrix} X_i \\ X_b \end{Bmatrix}=\begin{Bmatrix} X_i \\ \bar{H}_i \\ \hline X_b \end{Bmatrix}\cong\left[\begin{array}{c|c} \Phi_k & \Phi_c \\ \hline 0 & I \end{array}\right]\begin{Bmatrix} q_k \\ X_b \end{Bmatrix}, \qquad (k \ll n) \tag{12}$$

The original equations of vibration motion in Eq. (6) are transformed to Eq. (13) using Eq. (12). Transformed Eq. (13) can be greatly reduced in size from the original. Equation (13) is the CB model:

$$\begin{bmatrix} \omega_k^2 & \bar{K}_{kb} \\ \bar{K}_{kb}^T & \bar{K}_{bb} \end{bmatrix}\begin{Bmatrix} q_k \\ X_b \end{Bmatrix}+\begin{bmatrix} I & \bar{M}_{kb} \\ \bar{M}_{kb}^T & \bar{M}_{bb} \end{bmatrix}\begin{Bmatrix} \ddot{q}_k \\ \ddot{X}_b \end{Bmatrix}=0 \tag{13}$$

D. Coupling Equation

The DOFs of the solid-propellant model are connected with those of the motor case model using

$$\{X_b\}_j=\begin{Bmatrix} u_p \\ v_p \\ w_p \end{Bmatrix}_j=\begin{bmatrix} 1 & 0 & 0 & 0 \\ 0 & 1 & 0 & 0 \\ 0 & 0 & 1 & 0 \end{bmatrix}\begin{Bmatrix} u_c \\ v_c \\ w_c \\ \beta_c \end{Bmatrix}_i=[T_{ji}]\{X_c\}_i \tag{14}$$

The equation of the total SRM vibration motions can be obtained as expressed in Eq. (15) by coupling between Eq. (3) of the motor case and Eq. (13) of the propellant:

$$\begin{bmatrix} I & \bar{M}_{kb} \\ \bar{M}_{kb}^T & M_c+\bar{M}_{pp} \end{bmatrix}\begin{Bmatrix} \ddot{q}_k \\ \ddot{X}_c \end{Bmatrix}+\begin{bmatrix} \omega_k^2 & \bar{K}_{kb} \\ \bar{K}_{kb}^T & K_c+\bar{K}_{bb} \end{bmatrix}\begin{Bmatrix} q_k \\ X_c \end{Bmatrix}=0 \tag{15}$$

IV. Application of This Method

A. Generation of an Axial Vibration Model

An axial vibration model of an SRB with a length-to-radius ratio (L/R) of 7.8 was generated using the proposed simplified method described in Sec. III. Figure 6 shows the numerical model. The axial vibration model is derived from an axisymmetric vibration motion ($n=0$). The motor case model consists of 10 elements with uniform length and thickness. The solid-propellant model is divided into 3×10 elements.

The SRM mechanical properties are given in Table 1. A Poisson's ratio of 0.5 is used in the solid-propellant model. The coupling between the solid propellant and the motor case is expressed by Eq. (14a). The DOF of $\{u_p\}$ is constrained at each end of the propellant to move with the DOF $\{u_c\}$ of the motor case end:

$$\{X_b\}_j = \begin{Bmatrix} u_p \\ w_p \end{Bmatrix}_j = \begin{bmatrix} 1 & 0 & 0 \\ 0 & 1 & 0 \end{bmatrix} \begin{Bmatrix} u_c \\ w_c \\ \beta_c \end{Bmatrix}_i = [T_{ji}]\{X_c\}_i \qquad (14a)$$

The size of this simplified model of the SRM is 43 DOF, consisting of 33 for the motor case model physical DOF and 10 for the solid-propellant constrained normal modes. The effect of model division on the natural frequencies is presented in Table 2. Table 2 is a comparison of the natural frequencies in the free–free boundary condition obtained by 3×10 elements with those by 3×20 elements. This comparison suggests that the division of 3×10 is sufficiently accurate for the SRM axial vibration model. The effect of the number of constrained normal modes was found to be negligible, whether 10 or 20 modes were retained. Figure 7 shows the first four mode shapes obtained by the SRM model with 43 DOF.

Table 1 SRM mechanical properties

Property	Motor case	Solid propellant
Radius R, mm	Middle surface: 1250	Outer: 1250 Inner: 410
Length L	9750 mm	9750 mm
Thickness	15.0 mm	——
Elastic modulus	$E = 42.2$ GPa	$G = 27$ MPa
Poisson's ratio	0.3	0.5
Mass density	4.24 g/cm^3	1.8 g/cm^3

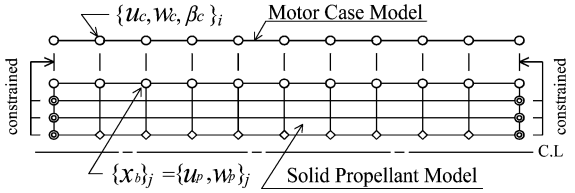

Fig. 6 Numerical model of an SRM.

B. Effects of Propellant Incompressibility

The simplified SRM model generation method proposed in Sec. III can treat the exact incompressibility of solid propellants with a Poisson's ratio of 0.5. However, there must be an approximated model generation method in which near incompressibility of a solid propellant is assumed to use the ordinary D-FEM. The approximated method uses a Poisson's ratio of 0.49 instead of 0.5. Therefore, the effects of incompressibility were analyzed for an SRM axial vibration in the free–free boundary condition. Table 3 lists the conditions for exact and approximated model generation of an SRM. The mechanical properties of the SRM are the same as those in Table 1, except for the solid propellant's Poisson's ratio of 0.49 in the approximated model. The convergence of natural frequencies vs the number of elements is shown in Fig. 8. Figure 8 indicates that the first three frequencies converge at 60 (3×20) and that the natural frequencies obtained by the exact model (Poisson's ratio of 0.5) are higher than those obtained by the approximated model (Poisson's ratio of 0.49). Table 4 is a comparison of the first three natural frequencies between the exact and approximated models at a

Table 2 Comparisons of natural frequencies (Hz)

Motor case propellant	10 division 3×10 division	20 division 3×20 division
First	50.71	50.94
Second	61.89	61.66
Third	77.07	76.09
Fourth	77.84	77.55
Fifth	90.82	89.76
Sixth	91.19	90.09

Table 3 Analysis conditions for SRM model generation

Property	Exact model	Approximated model	Coordinate system
		Motor case	
FEM	D-FEM	D-FEM	Physical
Model division	10, 20	10, 20	
		Solid propellant	
Poisson's ratio	0.5	0.49	Generalized number
FEM	M-FEM	D-FEM	of the constrained
Model division	3×10, 3×20, 6×20, and 8×20		normal modes = 20

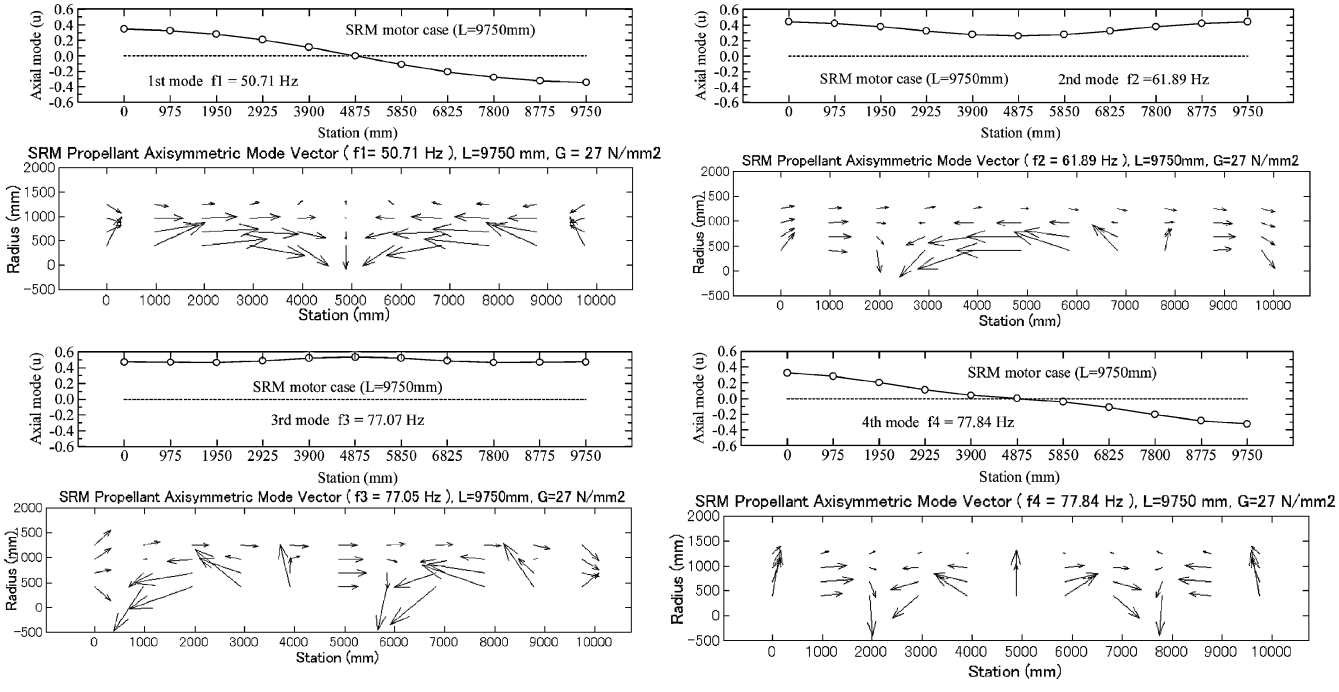

Fig. 7 Axial vibration mode shapes of the SRM ($L/R = 7.8$).

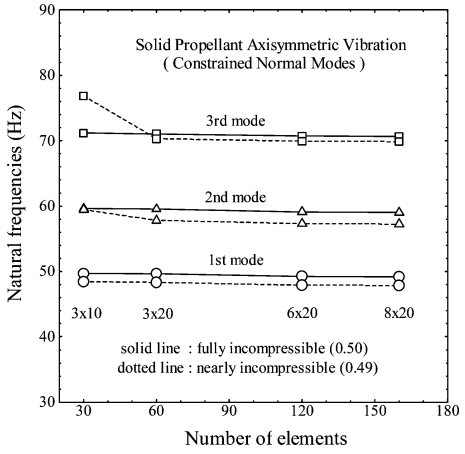

Fig. 8 Convergence of natural frequencies.

division of 60 (3 × 20). Figure 9 compares the corresponding mode shapes between the two models. The radial displacements along the inner surface of the solid propellant obtained by the two models are compared in Fig. 10 to clarify the difference between two models. Although the data in Table 4 suggest that effects of incompressibility on natural frequency are less than 3% and negligible for an SRB of $L/R = 7.8$, Figs. 9 and 10 indicate that those effects on mode shape are not negligible in terms of the SRM's structural dynamics.

Table 4 Comparison of natural frequencies of an SRM (Hz) (solid-propellant model: 3 × 20)

Mode	Exact model *a*	Approximate model *b*	*b*/*a*
1	50.94	49.61	0.974
2	61.66	60.33	0.978
3	76.09	75.96	0.998

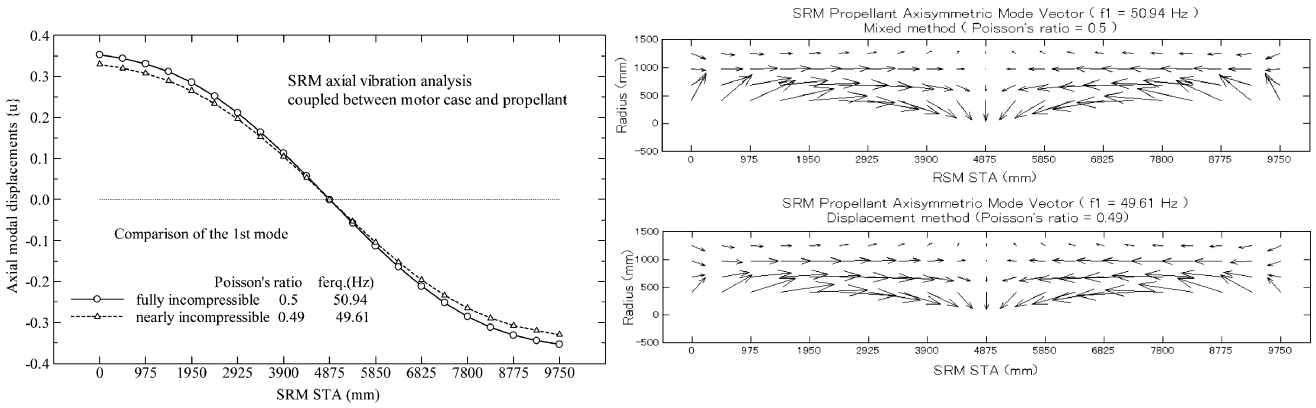

a) First mode of motor case and solid propellant

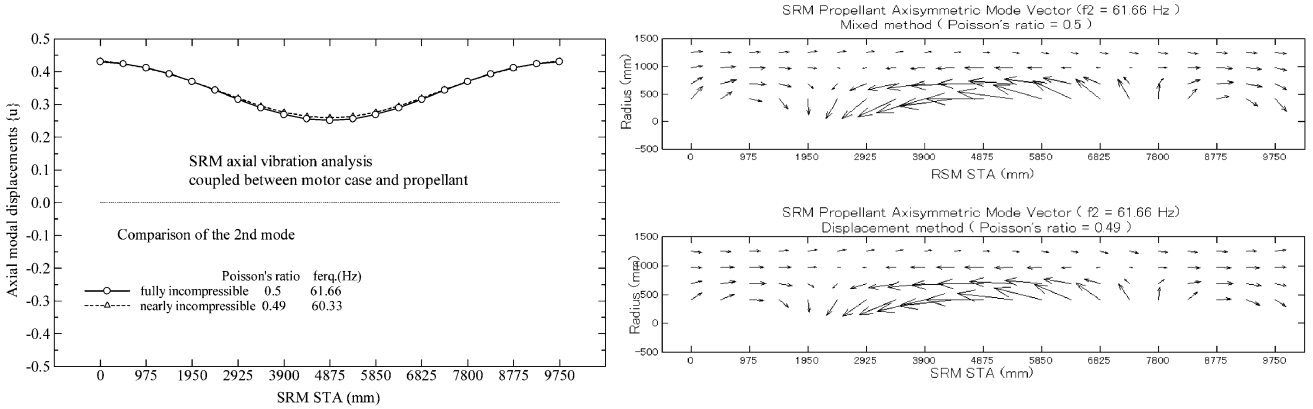

b) Second mode of motor case and solid propellant

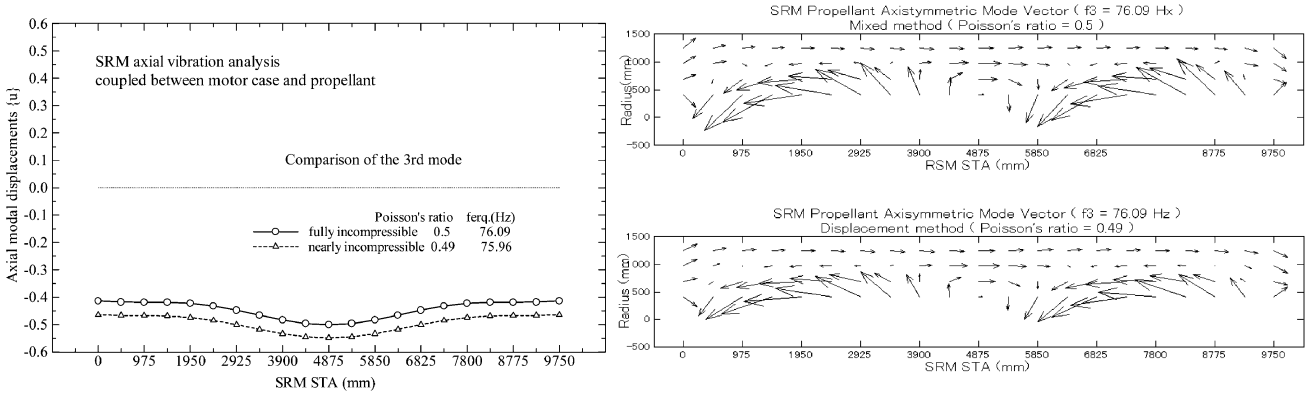

c) Third mode of motor case and solid propellant

Fig. 9 Comparison of mode shapes between $\nu = 0.5$ and 0.49.

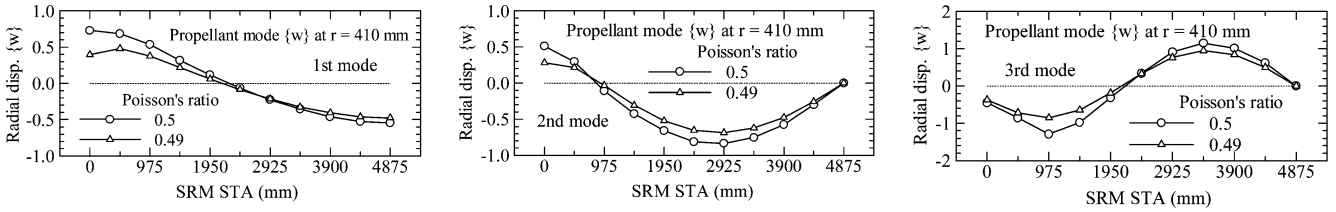

Fig. 10 Comparison of radial modes at the inner surface of a solid propellant between $\nu = 0.5$ and 0.49.

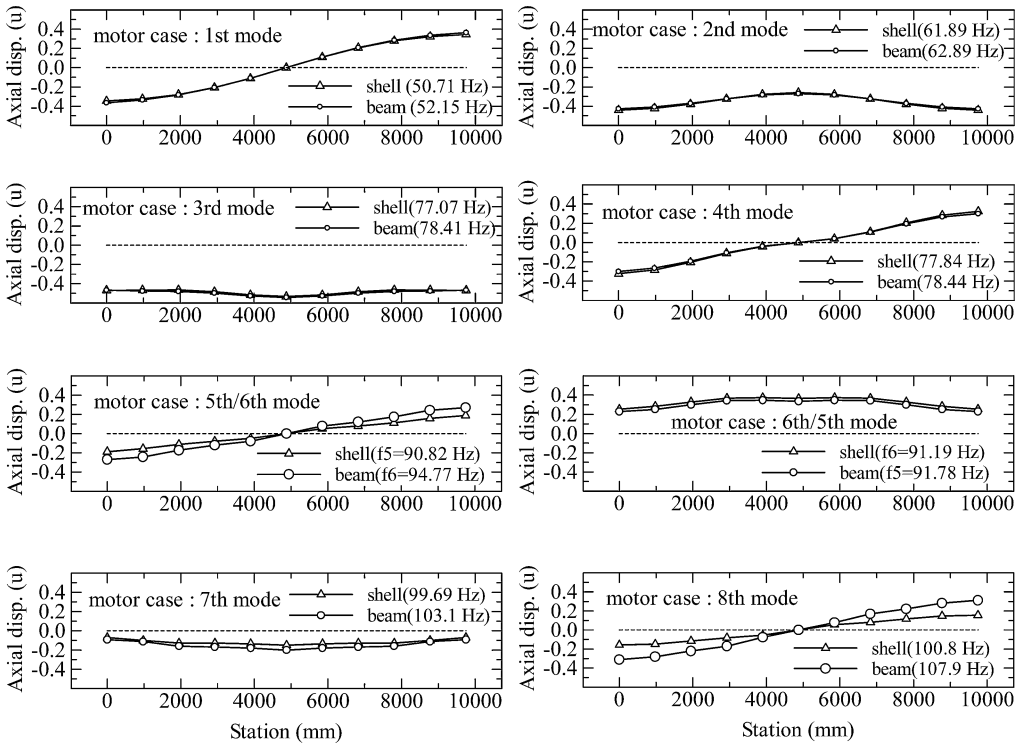

Fig. 11 Comparison of motor case axial modes between use of beam and shell model for motor case.

Table 5 Properties of the motor case beam model

Property	Beam model	Shell model (ref.)
Model division	10	10
Length	9750 mm	9750 mm
Radius	——	1250 mm
Thickness	——	15 mm
Stiffness	$AE = 5.0 \times 10^9$ N	$E = 42.2$ GPa
Poisson's ratio	——	0.3
Mass	0.5 kg/mm	$\rho = 4.24$ g/cm^3

Table 6 Comparison of natural frequencies (Hz) between use of beam and shell model for motor case

Mode	Beam a	Shell b	a/b
1	52.14	50.71	1.028
2	62.89	61.89	1.016
3	78.41	77.07	1.017
4	78.44	77.84	1.007
5	91.78[a]	90.82[b]	1.011
6	94.77[b]	91.19[a]	1.039
7	103.1	99.69	1.034
8	107.9	100.8	1.070

[a,b]Correspondence of normal mode shape.

C. Approximation of Motor Case Model

The incompressibility of solid propellant was assessed to be significant for the SRM axial vibration in Sec. IV.B. Further simplification was then analyzed for the motor case model from our standpoint of simplicity in model generation. One potential simplification is to replace the cylindrical shell theory with the beam theory to generate the motor case substructure model. The solid-propellant model and the motor case beam model are coupled by Eq. (14b):

$$\{X_b\}_j = \begin{Bmatrix} u_p \\ w_p \end{Bmatrix}_j = \begin{bmatrix} 1 \\ 0 \end{bmatrix} \{u_c\}_i = [T_{ji}]\{X_c\}_i \qquad (14b)$$

The axial vibration properties of the SRM using the beam theory were compared with those using the shell theory in the free–free boundary condition. Table 5 lists the mechanical properties of the motor case beam model, which correspond to those in Table 1. Comparisons of the natural frequencies are provided in Table 6. Comparisons of the motor case mode shapes are given in Fig. 11. The use of the beam theory contains two drawbacks. One is an order reversal with respect to the fifth and the sixth modes obtained by the use of the shell theory; the other is an appreciable difference in normal mode shape over the fifth mode. These results show that the beam model for the motor case substructure with an L/R ratio of 7.8 is simple and acceptable in the lower frequency range that is of interest in an SRM vibration analysis.

V. Conclusions

The purpose of this study was to propose a simplified vibration model of an SRM coupled with a solid propellant. The following

items were presented in this paper: 1) a simplified method for generating a structural vibration model of an SRM (Sec. III); 2) application of this method to generate an axial vibration mathematical model of an SRM (Sec. IV.A); 3) the SRM axial vibration properties analyzed based on the exact incompressible condition, that is, Poisson's ratio = 0.5, and on a near-incompressible condition, that is, Poisson's ratio = 0.49, for solid propellant (Sec. IV.B); and 4) comparisons between the beam model and shell model for the SRM case substructure (Sec. IV.C).

Our simplified model can treat the exact incompressibility (Poisson's ratio of 0.5) of solid propellant. This was confirmed with our exact algorithm for an eigenvalue calculation of the vibration motion of equations derived from the M-FEM. Effects of the propellant's incompressibility on the axial vibration behavior of an SRM with an L/R ratio of 7.8 proved to be significant. The axial vibration model was sufficiently accurate to be used as a beam model for a motor case substructure when coupled with a solid-propellant model of exact incompressibility. These findings confirm that our simplified vibration model of an SRM is simple and very reliable.

We are applying this method to generate a bending ($n = 1$, beam-type mode) and roll ($n = 0$) vibration model to be built into a vehicle vibration model. We also plan to verify this method experimentally.

Appendix: Summary of Eigenvalue Calculation Algorithm for Incompressible Materials

Equation (A1) expresses the vibration equation of motion for incompressible materials derived from the M-FEM. The zero diagonal elements in the system stiffness matrix produce numerical instability in full incompressibility (Poisson's ratio of 0.5):

$$\begin{bmatrix} M_{xx} & 0 \\ 0 & 0 \end{bmatrix} \begin{Bmatrix} \ddot{X} \\ 0 \end{Bmatrix} + \begin{bmatrix} K_{xx} & K_{xh} \\ K_{xh}^T & 0 \end{bmatrix} \begin{Bmatrix} X \\ H \end{Bmatrix} = 0 \qquad \text{(A1)}$$

where $\{X\}$ is the nodal displacement vector and $\{H\}$ is the nodal pressure vector.

Artificial compressibility, the penalty method, and the iteration method are techniques used to eliminate numerical instability in Eq. (A1). However, each technique is approximated because the value of Poisson's ratio may be 0.4999, not precisely 0.5. Given this situation, we developed an exact algorithm[6] that can conduct an eigenvalue analysis of Eq. (A1). This algorithm conducts the eigenvalue calculation after a specific coordinate transformation. This algorithm is summarized hereafter.

Equation (A2) defines the coordinate transformation:

$$\begin{Bmatrix} X \\ H \end{Bmatrix} = [\Phi]\{r\} \qquad \text{(A2)}$$

where $[\Phi]$ consists of the eigenvectors with a positive eigenvalue ($\lambda_i > 0$) obtained from the stiffness matrix in Eq. (A1). Here, $\{r\}$ refers to the orthogonal base coordinates that correspond to the positive eigenvalues. Transformation of Eq. (A1) using Eq. (A2) yields

$$[\bar{M}]\{\ddot{r}\} + \begin{bmatrix} \ddots & & \\ & \lambda & \\ & & \ddots \end{bmatrix} \{r\} = 0, \qquad [\bar{M}] = [\Phi]^T \begin{bmatrix} M_{xx} & 0 \\ 0 & 0 \end{bmatrix} [\Phi] \qquad \text{(A3)}$$

An eigenvalue analysis for ordinary vibration problems can be performed using the coordinate-transformed Eq. (A3). This algorithm, through which the numerical results obtained for axisymmetric vibrations of an incompressible cylinder converge with the analytical results, has been verified.[6]

References

[1]Herrmann, L. R., "Elasticity Equations for Incompressible and Nearly Incompressible Materials by a Variational Theorem," *AIAA Journal*, Vol. 3, No. 10, 1965, pp. 1896–1900.

[2]Zienkiewicz, O. C., and Taylor, R. L., "Incompressible Materials, Mixed Methods and Other Procedures of Solution," *The Finite Element Method, Volume 1 The Bases*, 5th ed., Butterworths, London, 2000, pp. 307–308.

[3]Hughes, T. J. R., *The Finite Element Method*, Dover, New York, 2000, pp. 192–231.

[4]Szabo, B., and Babuška, I., *Finite Element Analysis*, Wiley, New York, 1991, pp. 205–215.

[5]Zienkiewicz, O. C., and Taylor, R. L., "A Simple Iteration Process for Mixed Problems: Uzawa Method," *The Finite Element Method, Volume 1 The Bases*, 5th ed., Butterworths, London, 2000, pp. 323–325.

[6]Kohsetsu, Y., "An Algorithm Using Co-Ordinate Transformation for Free Vibration Analysis of Fully Incompressible Materials," *International Journal for Numerical Methods in Engineering*, Vol. 57, No. 5, 2003, pp. 669–684.

[7]Craig, R. R., Jr., and Bampton, M. C. C., "Coupling of Substructures for Dynamic Analysis," *AIAA Journal*, Vol. 6, No. 7, 1968, pp. 1313–1319.

[8]Bathe, K. J., *Finite Element Procedures*, Prentice–Hall, Englewood Cliffs, NJ, 1996, pp. 300–335.

[9]Washizu, K., *Variational Methods in Elasticity*, 2nd ed., Pergamon, New York, 1975, pp. 358–360.

L. Peterson
Associate Editor